



Published in final edited form as:

J Med Chem. 2021 September 23; 64(18): 13893–13901. doi:10.1021/acs.jmedchem.1c01289.

α /Sulfono- γ -AApeptide Hybrid Analogues of Glucagon with Enhanced Stability and Prolonged In Vivo Activity

Peng Sang[▽],

Department of Chemistry, University of South Florida, Tampa, Florida 33620, United States

Hongxiang Zeng[▽],

Institute of Life Sciences, Chongqing Medical University, Chongqing 400016, China

Candy Lee[▽],

Calibr at Scripps Research, La Jolla, California 92037, United States

Yan Shi,

Department of Chemistry, University of South Florida, Tampa, Florida 33620, United States

Minghui Wang,

Department of Chemistry, University of South Florida, Tampa, Florida 33620, United States

Cong Pan,

Department of Chemistry, University of South Florida, Tampa, Florida 33620, United States

Lulu Wei,

Department of Chemistry, University of South Florida, Tampa, Florida 33620, United States

Chenglong Huang,

Institute of Life Sciences, Chongqing Medical University, Chongqing 400016, China

Mingjun Wu,

Institute of Life Sciences, Chongqing Medical University, Chongqing 400016, China

Weijun Shen,

Calibr at Scripps Research, La Jolla, California 92037, United States

Xi Li,

Institute of Life Sciences, Chongqing Medical University, Chongqing 400016, China

Corresponding Authors: Weijun Shen – wshen@scripps.edu, Xi Li – lixi@cqmu.edu.cn, Jianfeng Cai – jianfengcai@usf.edu.

[▽]P.S., H.Z., and C.L. contributed equally to this work.

Author Contributions

J.C., X.L., and W.S. directed the experiments. P.S., H.Z., C.L., and Y.S. conducted the experiments. P.S., J.C., X.L., and W.S. performed data analysis. P.S. and J.C. wrote the manuscript draft. All authors contributed to discussing the data and proofreading the manuscript.

The authors declare no competing financial interest.

ASSOCIATED CONTENT

Supporting Information

The Supporting Information is available free of charge at <https://pubs.acs.org/doi/10.1021/acs.jmedchem.1c01289>.

Additional schemes and figures; HPLC traces; HRMS spectra of compounds; and NMR spectra of the sulfono- γ -AA peptide building blocks (PDF)

Molecular formula strings (CSV)

Complete contact information is available at: <https://pubs.acs.org/doi/10.1021/acs.jmedchem.1c01289>

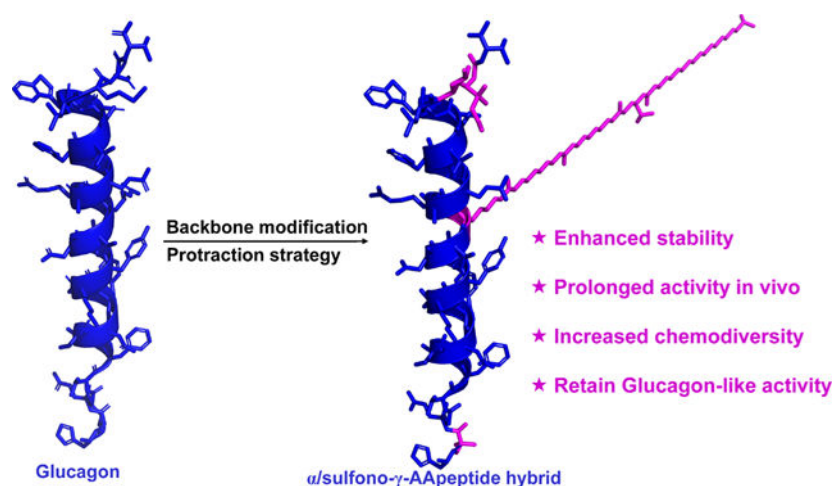
Jianfeng Cai

Department of Chemistry, University of South Florida, Tampa, Florida 33620, United States

Abstract

Peptide drugs have the advantages of target specificity and good drugability and have become one of the most increasingly important hotspots in new drug research in biomedical sciences. However, peptide drugs generally have low bioavailability and metabolic stability, and therefore, the modification of existing peptide drugs for the purpose of improving stability and retaining activity is of viable importance. It is known that glucagon is an effective therapy for treating severe hypoglycemia, but its short half-life prevents its wide therapeutic use. Herein, we report that combined unnatural residues and long fatty acid conjugation afford potent α /sulfonyl- γ -AApeptide hybrid analogues of Glucagon with enhanced stability and prolonged in vivo activity. This strategy could be adopted to develop stabilized analogues of other short-acting bioactive peptides.

Graphical Abstract



INTRODUCTION

Recently, bioactive peptides have been more intensely explored for the development of new drug candidates and/or molecular probes because of their unique and attractive characteristics, such as significant activity, excellent specificity, and low toxicity.^{1,2} However, their short in vivo half-lives, poor membrane permeability, and inferior bioavailability have remained paramount challenges. Among recent advances, backbone modification has emerged as an effective strategy using unnatural residues such as β -amino acids^{3–6} or oligoureas⁷, to replace a few α -amino acid residues in short-acting bioactive peptides in order to achieve enhanced resistance to proteolytic degradation, more favorable pharmacokinetic (PK) properties, and retain biological activity in vivo. As proteolytically stable peptidomimetics, sulfonyl- γ -AApeptides (Figure 1) exhibit remarkable capability of mimicking the helical domain of proteins and modulating a range of medically relevant protein–protein interactions (PPIs).^{9–14} Indeed, helical sulfonyl- γ -AApeptides, including left-handed^{12–14} and right-handed¹¹ homogeneous sulfonyl- γ -AApeptides, as well as left-

handed and right-handed 1:1 heterogeneous α /sulfono- γ -AApeptides,^{9,15–17} have been demonstrated as suitable backbones for mimicking the helical domain of bioactive peptides owing to their robust helical folding propensity and close similarity to α -helix; however, the replacement of just a few canonical amino acid residues in the long bioactive peptides with unnatural sulfono- γ -AA residues remains rather underexplored.¹⁸

It is known that a sulfono- γ -AA residue is comparable to a dipeptide residue in length (Figure 1), and our previous studies also demonstrated that 1:1 α /sulfono- γ -AA repeats lead to well-defined 4_{13} helix.¹⁰ In addition, these 1:1 α /sulfono- γ -AA patterned hybrid peptides are completely resistant to proteolysis.⁹ However, considering the unique spatial arrangement and electronic properties of sulfono- γ -AA residues, their suitability as minimal inserts in canonical long peptides for generating more potent and more proteolytically stable α /sulfono- γ -AA peptide hybrids was unrevealed and encountered several potential challenges. In the specific case of using a sulfono- γ -AA residue (Figure 1B,C) as an insert, it was unclear if the overall configuration of the peptide could be impacted. Would the position of the sulfono- γ -AA residue insert also affect the three-dimensional structure of the peptide and its function? Whether or not can the minor backbone modification help improve stability? Additional uncertainty might arise from potential H-bonding interactions between the sulfono- γ -AA residue and the neighboring α amino acid units; such a new interaction may also affect the activity of the hybrid peptide. We felt that it would be meaningful to explore the strategy of minimal sulfono- γ -AA residue insertion in bioactive peptides if the resulted peptide hybrids show improved stability and activity as their synthesis would be considerably more straightforward compared with homogeneous and 1:1 heterogeneous sulfono- γ -AApeptides because the sequences are still mainly based on canonical amino acids. In addition, it would be virtually impossible for any class of unnatural foldamers with the entire unnatural backbone to mimic long helical peptides because there are always differences in helical folding parameters between unnatural peptidomimetics and α -helix. The strategy of minimal insertion of sulfono- γ -AA residues into long bioactive peptides may have a better probability to retain the activity and enhance the stability, although at the sacrifice of proteolytic resistance compared to homogeneous sulfono- γ -AApeptides.

Glucagon is an essential hormone for regulating glucose homeostasis and acts as a counter-regulatory hormone for insulin.²⁰ Unlike GLP-1, which stimulates glucose uptake, glucagon essentially binds to a glucagon receptor (GCGR) and increases glucose concentration in the blood stream. The increase in circulating glucose levels is achieved by stimulating liver glucose production by increasing glycogenolysis and gluconeogenesis under fasting conditions. It is considered an effective therapy for treating severe hypoglycemia; however, its plasma half-life is very short (in a couple of minutes), which limits its wide clinical applications.^{21–24} Interestingly, although noticeable effort has been extended to develop GLP-1 analogues with improved stability,^{25–27} there are very few reports on developing stabilized analogues of glucagon, even though the development of proteolytically stable glucagon analogues could be considerably significant in biomedical sciences.²⁸ To explore the potential applications of α /sulfono- γ -AApeptide hybrids using minimal insertion of sulfono- γ -AA residues for stabilizing short-acting bioactive peptides, we chose this long and complex helical glucagon peptide as the target. We attempted to swap α amino acids with sulfono- γ -AA and other unnatural residues and also combine the protraction

strategy,^{25,29–31} which involves functionalizing peptides with polyethylene glycol (PEG) and long fatty acid chains to promote binding to albumin and prolong in vivo activity, in the hope of developing glucagon analogues with enhanced stability and prolonged biological activity. If successful, it would offer a new and alternative strategy for developing stabilized analogues of short-acting bioactive peptides.

RESULTS AND DISCUSSION

Design of α /Sulfono- γ -AApeptide Hybrids.

Our α /sulfono- γ -AApeptide hybrids design was based on glucagon-NH₂ and started with the introduction of sulfono- γ -AA residues from the C terminus of glucagon (Table 1 and Figure 2A).³² As alternative α -amino acid and L-sulfono- γ -AA hybrid peptide in a 1:1 repeat pattern forms a robust 4₁₃ helical structure (pitch: 5.5 Å) similar to α -helix (right-handed 4₁₃ helix, pitch 5.4 Å),^{15–17} the replacement of three neighboring amino acids with one amino acid and one sulfono- γ -AA residue was expected to retain the helix structure in glucagon (Figure 2B). In addition, it is widely known that inclusion of addition unnatural amino acids and long PEG and fatty acid chains (Figure 2C) was also manifested to enhance the stability and activity.^{26,31} The activity of these α /sulfono- γ -AApeptide hybrids **1–10** (Table 1) was first determined using a cAMP response element (CRE)-driven luciferase reporter in human embryonic kidney (HEK) (HEK293) cells stably expressing human GCGR obtained with **O8** as the control³³ (Figure 3). Sequence **1**, in which one sulfono- γ -AA residue **X**¹ was used to substitute methionine (Met) and asparagine (Asn) residues in glucagon, as well as its N-terminal acetyl-capped counterpart **2** showed excellent activity in activating GCGR. It is exciting that sequence **1** has even more potent activity than **O8**, suggesting that the inclusion of sulfono- γ -AA residue **X**¹ at the C-terminal of glucagon could be potentially valuable. It is interesting that acetylation of N-terminal histidine residue did not strongly affect the activity because **2** is only ~ threefold weaker than **1**. However, peptides **3–10**, bearing 2 to 5 sulfono- γ -AA residues in lieu of corresponding amino acid residues, had entirely lost their activity. The insertion of two sulfono- γ -AA peptide residues, with one being kept at the C-terminal and the other one being in the center, also did not exhibit any activity (Table 1, **11–12**). This may imply that the inclusion of more than one sulfono- γ -AA residue could alter the overall configuration of the glucagon sequence. We therefore decided to use sequence **1** as the lead for further development. Next, we introduced unnatural residues at position 2 of glucagon in lieu of L-serine to prevent possible dipeptidyl peptidase-4 (DPP-4) degradation on glucagon and GLP-1 peptide derivatives (Table 1, **13–16**).^{27,34} Although the use of Glycine at position 2 led to loss of some activity, Aib at the same position retained the potent activity (Table 1, **15** and **16**). In addition, we introduced the protraction strategy³⁵ to add a long fatty acid chain (Figure 2A) to the peptide backbone in the hope of improving in vivo PK properties (Table 1, **17–19**). The position of the fatty acid chain was likely to have great influence on the activity of derivatives of **15** bearing the Aib2 residue, as seen for sequences **17**, **18**, and **19**. The fatty acid chain appended to K20 significantly abolished the activity, and **18** even completely lost the activity with a fatty acid chain attached to K24 (Table 1 and Figure 3). The sequence **19**, bearing the attachment of the fatty acid chain onto K17, seemed to have the least reduction in the activity. To avoid the interference of the serum-binding fatty acid on the agonistic activity, we have also developed

a cAMP assay by measuring the receptor-mediated cAMP production with a homogeneous time-resolved fluorescence (HTRF) kit in Chinese hamster ovary (CHO)-K1 cells in the absence of fetal bovine serum (FBS) using glucagon as the positive control (Figure 4). To our satisfaction, the results can be mutually verified with the aforementioned Cre-luciferase (Luc) production functional assays (Table 1 and Figure 3), and results from both assays matched almost perfectly.

Circular Dichroism Studies.

Circular dichroism (CD) spectroscopy was next used to determine the secondary structures of regular glucagon peptides and α /sulfonyl- γ -AApeptide hybrid analogues in solution in the range of 195–260 nm (Figure 5). The results revealed that these peptides adopt similar right-handed α -helix at 100 μ M concentration in phosphate-buffered saline (PBS), which is supported by the double minimum at 205 and 225 nm. Indeed, compared with glucagon, majority of the α /sulfonyl- γ -AApeptide hybrid revealed the most pronounced negative signatures, implying that the inclusion of the sulfonyl- γ -AA residue enhanced the helicity of the peptides. It may also be the reason why the lead compounds can still maintain good activity.

Modeling Studies.

We then performed structural analysis of the lead compound **19** by computer modeling using the PyMOL software (Figure 6). α /Sulfonyl- γ -AApeptide hybrid **19** was overlaid with the glucagon helical structure (PDB: 1GCN) and revealed that most of its critical side chains could align with the side chains of native glucagon (Figure 6A,C). The change from M27N28 to X¹ at the N-terminus has no significant effect on the configuration of the whole skeleton. Replacing Arg with K^{Tail} at position **17** also does not affect other surrounding residues.

In Vitro Human Serum Stability Studies.

Clinical applications of many biologically and pharmacologically interesting peptide-based drugs have been restricted by poor stability of unmodified peptides against proteolysis. To determine if the α /sulfonyl- γ -AApeptide hybrid analogues could enhance stability, we next performed serum stability studies of the lead compound **19** in comparison to the regular glucagon peptide (Figure 6D,E). Each peptide was incubated in human serum at 37 °C for 24 h. The sample was then measured by reversed-phase high-performance liquid chromatography (RP-HPLC) to analyze the stability of the examined peptides. The lead α /sulfonyl- γ -AApeptide hybrid **19** showed no detectable degradation (Figure 6E), whereas the regular glucagon exhibited more than 85% degradation under the same condition (Figure 6D), which indicates that the designed α /sulfonyl- γ -AApeptide hybrid could improve the stability toward proteolytic degradation.

In Vivo Studies.

We then conducted in vivo studies using two sets of mice to further validate our design (Figure 7). With the best lead compounds **15** and **19** in hand, we chose them for the pharmacokinetic experiment in mice with glucagon being included as the control (Figure

7A). Consistent with previous findings,³⁶ glucagon was metabolized quickly and was not found in blood after 15 min. Intriguingly, with the inclusion of one Aib and one sulfono- γ -AA residue, the sequence **15** showed improved in vivo stability, as it was still detectable at 30 min time point (Figure 7A), suggesting that even minimal insertion of unnatural residues could have an impact on the metabolic stability of the peptide. As anticipated, the lead compound **19**, which combined unnatural residues and long fatty acid conjugation, showed much more enhanced stability compared with glucagon, and the lead linear α /sulfono- γ -AApeptide hybrid analogue **15** exhibited a significant increase in half-life (~4 h, Figure 7A). Subsequently, the abilities of glucagon, **15** and **19**, to increase blood glucose were evaluated by intraperitoneal insulin tolerance test (IPITT) in C57BL/6J female mice. As shown in Figure 7B, female mice that received glucagon, including both low (Glucagon-L) and high doses (glucagon-H), have higher blood glucose during the whole experiment. It is also noteworthy that although initially high dose of glucagon elicited higher glucose levels in the blood stream, after 30 min, the effect of both low and high doses exhibited comparable efficacy. Interestingly, both low (**15-L**) and high doses (**15-H**) of sequence **15** showed virtually the same efficacy to stimulate glucose release, which is somewhat similar to the behaviors of glucagon. It is noted that **19**, which bears a long fatty acid chain and exhibits less potent activity than **15**, could boost stronger glucose release than **15** and only displayed slightly reduced potency compared with glucagon (Figure 7B) at the high dose (**19-H**). Unlike other two compounds, it seems that the high dose of **19** (**19-H**) is always more effective than the low dose (**19-L**) up to 60 min under the tested conditions. The overall results revealed that our lead compounds showed excellent activity and enhanced stability, which is consistent with the results of in vitro experiments.

CONCLUSIONS

In summary, we have developed a series of α /sulfono- γ -AApeptide hybrids to modify and modulate the properties of glucagon based on backbone modification and the protraction strategy. The strategy is highlighted with enhanced stability and prolonged activity in vivo, allowing for retaining native glucagon-like activity. This work represents, to date, the first successful example for the stabilization of glucagon using sulfono- γ -AA residues. This novel backbone modification approach may be useful for developing peptides with therapeutic potential, and the exploration of this strategy to develop stabilized analogues of other short-acting bioactive peptides is currently underway in our laboratory.

EXPERIMENTAL SECTION

General Information.

Proton nuclear magnetic resonance (¹H NMR) spectra and carbon nuclear magnetic resonance (¹³C NMR) spectra were recorded on a Bruker 400-MHz instrument. Chemical shifts for protons are internally referenced to residual (CH₃)₂SO signals (δ 2.5 ppm). Data are reported as follows: chemical shift (δ ppm), integration, multiplicity (s = singlet, d = doublet, dd = doublet of doublets, t = triplet, q = quartet, br = broad, and m = multiplet), and coupling constants (Hz). Chemical shifts for carbon are reported in ppm with residual (CH₃)₂SO as the internal standard (δ 39.00 ppm). High-resolution mass spectrometry

(HRMS) data were obtained on an Agilent 1100 LC/MS ESI/TOF mass spectrometer with electrospray ionization. Solid-phase synthesis of the peptides was conducted in the peptide synthesis vessels on a Burrell Wrist-Action shaker. All peptides were analyzed and purified on a Waters Breeze 2 HPLC system installed with both an analytic module (1 mL/min) and a preparative module (16 mL/min) by employing a method using 5–100% linear gradient of solvent B (0.1% TFA in MeCN) in solvent A (0.1% TFA in H₂O) over 50 min, followed by 100% solvent B over 15 min. The desired peptides were collected and lyophilized on a Labcono lyophilizer, and the purity was determined to be >95% by analytical HPLC.

Solvents as well as other commercial reagents were purchased from Sigma-Aldrich, Acros, Alfa Aesar, Oakwood Products Inc., TCI, GL Biochem (Shanghai, China), or Chem-Impex (Wood Dale, IL) and used as received unless otherwise stated. Thin-layer chromatography (TLC) was performed on SorBent Tech. TLC plates (silica gel 60 F254). Flash column chromatography was performed with SorBent Tech. silica gel (60 Å, 230–400 mesh, 32–63 μ m).

Preparation of Sulfonyl- γ -AA Building Blocks.

Sulfonyl- γ -AApeptide building blocks **1a–e** (Figure S1) were synthesized according to the reported procedure (Schemes S1 and S2).^{12–14} Fmoc-protected amino acids (Fmoc-AA-OH) were used as the initial starting materials.

(S)-N-(2-((((9H-fluoren-9-yl)methoxy)carbonyl)amino)-5-(3-((2,2,4,6,7-pentamethyl-2,3-dihydrobenzofuran-5-yl)-sulfonyl)guanidino)pentyl)-N-(methylsulfonyl)glycine (**1a**).

¹H NMR (400 MHz, DMSO-*d*₆): δ 7.84 (d, *J* = 7.20 Hz, 2H), 7.65 (d, *J* = 6.80 Hz, 2H), 7.36 (t, *J* = 7.20 Hz, 2H), 7.29 (d, *J* = 5.20 Hz, 2H), 7.14 (d, *J* = 8.80 Hz, 1H), 6.39–6.66 (m, 2H), 4.27–4.31 (m, 3H), 4.18 (t, *J* = 6.40 Hz, 2H), 3.95 (s, 2H), 3.61 (brs, 1H), 3.22–3.26 (m, 1H), 3.08–3.14 (m, 1H), 3.00 (brs, 2H), 2.90 (s, 5H), 2.47 (s, 3H), 2.40 (s, 3H), 1.97 (s, 3H), 1.50 (brs, 1H), 1.35 (s, 6H), 1.19–1.25 (m, 2H). ¹³C NMR (100 MHz, DMSO-*d*₆): δ 171.2, 157.9, 156.4, 144.3, 141.2, 137.7, 134.6, 131.9, 128.0, 127.5, 125.6, 124.8, 120.5, 116.7, 86.7, 65.6, 51.5, 50.0, 48.8, 47.3, 42.9, 29.7, 28.7, 19.4, 18.0, 12.7. HRMS (ESI) ([M + H]⁺) Calcd. for C₃₇H₄₇N₅O₉S₂: 769.2815, found: 770.2904.

(S)-N-(2-((((9H-fluoren-9-yl)methoxy)carbonyl)amino)-6-((tert-butoxycarbonyl)amino)hexyl)-N-((4-chlorophenyl)-sulfonyl)glycine (**1b**).

¹H NMR (400 MHz, DMSO-*d*₆): δ 7.84 (d, *J* = 7.20 Hz, 2H), 7.74 (d, *J* = 8.40 Hz, 2H), 7.63 (d, *J* = 7.20 Hz, 2H), 7.56 (*J* = 8.40 Hz, 2H), 7.315–7.37 (m, 2H), 7.26–7.30 (m, 2H), 7.06 (d, *J* = 8.40 Hz, 1H), 6.70 (brs, 1H), 4.16–4.23 (m, 3H), 3.99 (q, *J* = 29.2, 1 8.40 Hz, 2H), 3.54 (brs, 1H), 3.23 (dd, *J* = 14.40, 5.60 Hz, 1H), 3.11 (q, *J* = 14.00, 8.00 Hz, 1H), 2.83 (d, *J* = 5.60 Hz, 2H), 2.46 (s, 1H), 1.39 (brs, 1H), 1.32 (s, 9H), 1.11–1.28 (m, 4H). ¹³C NMR (100 MHz, DMSO-*d*₆): δ 170.3, 156.2, 156.0, 144.3, 144.2, 141.1, 138.9, 138.0, 129.6, 129.3, 128.0, 127.4, 125.6, 120.5, 77.7, 65.6, 52.0, 49.9, 48.8, 47.2, 31.7, 29.8, 28.7, 23.1. HRMS (ESI) ([M + H]⁺) Calcd. for C₃₄H₄₀ClN₃O₈S: 685.2225, found: 686.2302. 34 40 38

(S)-N-(2-(((9H-fluoren-9-yl)methoxy)carbonyl)amino)-4(tert-butoxy)-4-oxobutyl)-N-((4-chlorophenyl)sulfonyl)glycine (1c).

¹H NMR (400 MHz, DMSO-*d*₆): δ 7.84 (d, *J* = 7.20 Hz, 2H), 7.75 (d, *J* = 8.40 Hz, 2H), 7.62 (d, *J* = 7.60 Hz, 2H), 7.57 (d, *J* = 8.40 Hz, 2H), 7.37 (t, *J* = 7.20 Hz, 2H), 7.27 (t, *J* = 5.60 Hz, 2H), 7.20 (d, *J* = 8.80 Hz, 1H), 4.15–4.21 (m, 3H), 4.01 (q, *J* = 38.40, 18.80 Hz, 3H), 3.27 (dd, *J* = 14.40, 6.00 Hz, 1H), 3.17 (q, *J* = 14.00, 8.00 Hz, 1H), 2.50 (d, *J* = 4.80 Hz, 1H), 2.29 (q, *J* = 15.20, 8.80 Hz, 1H), 1.32 (s, 9H). ¹³C NMR (100 MHz, DMSO-*d*₆): δ 170.3, 170.1, 155.8, 144.2, 141.1, 138.7, 138.1, 129.7, 129.3, 128.0, 127.4, 125.6, 120.5, 80.4, 65.9, 51.3, 49.0, 47.2, 47.1, 38.4, 28.1. HRMS (ESI) ([M + H]⁺) Calcd. for C₃₁H₃₃ClN₂O₈S: 628.1646, found: 629.1734.

(S)-N-(2-(((9H-fluoren-9-yl)methoxy)carbonyl)amino)-4methylpentyl)-N-((2-((tert-butoxycarbonyl)amino)ethyl)-sulfonyl)glycine (1d).

¹H NMR (400 MHz, DMSO-*d*₆): δ 7.83 (d, *J* = 7.20 Hz, 2H), 7.65 (t, *J* = 5.60 Hz, 2H), 7.37 (t, *J* = 7.20 Hz, 2H), 7.28 (d, *J* = 3.20 Hz, 2H), 7.14 (d, *J* = 8.80 Hz, 1H), 6.85 (brs, 1H), 4.30 (d, *J* = 5.60 Hz, 2H), 4.17 (t, *J* = 6.40 Hz, 1H), 3.98 (s, 2H), 3.69 (brs, 1H), 3.23–3.29 (m, 5H), 3.08–3.14 (m, 1H), 1.53 (brs, 1H), 1.32 (s, 9H), 1.16–1.26 (m, 2H), 0.81 (q, *J* = 11.20, 6.40 Hz, 6H), 0.69–0.75 (m, 1H). ¹³C NMR (100 MHz, DMSO-*d*₆): δ 171.2, 156.3, 155.7, 144.4, 144.2, 141.2, 128.0, 127.4, 125.6, 120.5, 78.5, 65.6, 51.9, 51.6, 48.7, 48.2, 47.3, 41.2, 35.2, 28.6, 24.6, 23.7, 22.0. HRMS (ESI) ([M + H]⁺) Calcd. for C₃₀H₄₁N₃O₈S: 603.2614, found: 604.2700.

(S)-N-(2-(((9H-fluoren-9-yl)methoxy)carbonyl)amino)-4(tert-butoxy)-4-oxobutyl)-N-((2-((tert-butoxycarbonyl)amino)-ethyl)sulfonyl)glycine (1e).

¹H NMR (400 MHz, DMSO-*d*₆): δ 7.85 (d, *J* = 7.60 Hz, 2H), 7.63 (t, *J* = 6.80 Hz, 2H), 7.37 (t, *J* = 7.60 Hz, 2H), 7.28 (t, *J* = 7.20 Hz, 3H), 6.86 (brs, 1H), 4.25 (d, *J* = 6.80 Hz, 2H), 4.16 (t, *J* = 6.40 Hz, 1H), 3.95 (q, *J* = 30.8, 18.80 Hz, 3H), 3.16–3.26 (m, 6H), 2.48 (t, *J* = 5.60 Hz, 1H), 2.27 (q, *J* = 15.60, 8.80 Hz, 1H), 1.32 (s, 18H). ¹³C NMR (100 MHz, DMSO-*d*₆): δ 171.1, 170.1, 156.0, 155.7, 144.2, 141.1, 128.0, 127.5, 125.6, 120.5, 80.4, 78.5, 65.9, 51.5, 50.8, 48.7, 47.1, 38.4, 35.1, 28.6, 28.1. HRMS (ESI) ([M + H]⁺) Calcd. for C₃₂H₄₃N₃O₁₀S: 661.2669, found: 662.2761.

Synthesis of Glucagon Analogues.

Glucagon and α/sulfono-αAapeptide hybrid analogues were synthesized using 100 mg of Rink amide-4-methylbenzhydrylamine (MBHA) resin (0.646 mmol/g) at room temperature under air. The resin was swelled in dimethylformamide (DMF) for 5 min before use, followed by treatment with 20% piperidine/DMF solution (2 mL) for 15 min (×2) to remove the Fmoc-protecting group, afterward washed with dichloromethane (DCM) (×3) and DMF (×3). A premixed solution of the Fmoc-protected regular amino acid/sulfono-γ-AApeptide building block (2 equiv), 1-hydroxybenzotriazole (HOBt) (4 equiv), and *N,N'*-diisopropylcarbodiimide (DIC) (4 equiv) in 2 mL of DMF was added to the resin and shaken for 2–4 h to complete the coupling reaction. After washing with DCM and DMF, the resin was treated with 20% piperidine/DMF solution for 15 min (×2), afterward washed with DCM (×3) and DMF (×3). Another Fmoc-protected regular amino acid/sulfono-γ-

AApeptide building block (2 equiv) was attached onto the resin, following the procedure in the first coupling step, and the Fmoc-protecting group was removed after the coupling reaction was performed. The reaction cycles were repeated until the desired sulfono- γ -AApeptides were synthesized. For the capped sequence, the N-terminus was treated with 1 mL of acetic anhydride in 2 mL of pyridine (15 min \times 2).

The general coupling procedure for the peptide tail on the solid phase is as follows: acid (3 equiv), [bis(dimethylamino)methylene]-1*H*-1,2,3-triazolo[4,5-*b*]pyridinium 3-oxid hexafluorophosphate (HATU) (3.3 equiv), and *N,N*-Diisopropylethylamine (DIPEA) (3.3 equiv) in DMF for 4 h (acid = Fmoc-OcO₂-OH, N-Fmoc-Glu (OH)-OtBu, or 18-(ter-butoxy)18-oxooctadecanoic acid).

The cleavage was conducted using a cocktail of trifluoroacetic acid/phenol/water/thioanisole/1,2-ethanedithiol (4 mL, 82.5:5:5:5:2.5, v/v) for 2.5 h at room temperature. The resin was then filtered, and the filtrate was precipitated using 40 mL of cold ethyl ether. Following precipitation, the crude peptide was spun down on a centrifuge for 15 min at 4500 rcf. The supernatant was removed, and the crude product was analyzed and purified using the Waters HPLC system.

In Vitro Assays.

CRE-Luciferase Reporter Assay.—For monitoring the activation of GCGR, stable HEK cell lines with the human GCGR overexpression were introduced together with CRE-responsive firefly luciferase reporter using lentivirus and selected with puromycin (1 μ g/mL) and G418 (1 mg/mL). HEK293 cells that stably overexpressed GCGR with the CRE-responsive firefly luciferase reporter were stimulated with glucagon as the positive control and the peptide samples for 16 h at 37 °C, 5% CO₂. After 16 h of stimulation, cells were added to the luciferase detection reagent (Bright-Glo Reagent, Promega). The luminescence signal was measured on a ViewLux (PerkinElmer) immediately. The values of half-maximal effective concentration (EC₅₀) were obtained using the Prism software.

Intracellular cAMP Assay.—Test cell line generation: Human GCGR complementary deoxyribonucleic acid (cDNA) clone was synthesized. Transient transfections of HEK293 and CHO-K1 cells were performed using Lipofectamine 2000 and selected with G-418 (300 μ g/mL for HEK; 1000 μ g/mL for CHO-K1) for stable cell lines. For monitoring the direct activity of cAMP activity, the stable CHO-K1 cell lines with hGCGR overexpression were used. CHO-K1 cells that stably overexpressed hGCGR were stimulated with glucagon as positive control and the peptide samples for 30 min at 37 °C, 5% CO₂. After 30 min, cells were added to the cAMP detection reagent (cAMP-GS Dynamic Kit, cisbio). The HTRF signal was measured on ViewLux (Perkin Elmer) immediately. The values of EC₅₀ were obtained using the Prism software.

CD Spectroscopy.—CD spectra were measured on an Aviv 215 CD spectrometer using a 1 mm path length quartz cuvette, and compound solutions in PBS buffer were prepared using the dry weight of the lyophilized solid, followed by dilution to give the desired concentration (100 μ M) and solvent combination. Ten scans were averaged for each sample, and 3 times of independent experiments were conducted, and the spectra were averaged. The

final spectra were normalized by subtracting the average blank spectra. Molar ellipticity $[\theta]$ ($\text{deg}\cdot\text{cm}^2\cdot\text{dmol}^{-1}$) was calculated using the following equation:

$$[\theta] = \theta_{\text{obs}} / (n \times l \times c \times 10)$$

where θ_{obs} is the measured ellipticity in millidegrees, while n is the number of side groups, l is the path length in centimeter (0.1 cm), and c is the concentration of the compound in molar unit.

In Vitro Human Serum Stability Assay.—The serum stabilities of peptides were determined in 25% (v/v) aqueous-pooled serum from human male AB plasma.³⁷ Peptides were diluted in serum at a final concentration of 2 mg/mL and incubated at 37 °C for 24 h. The solution (50 μL) was added to 50 μL of acetonitrile (ACN) on ice for 20 min, and then, it was centrifuged at 4 °C for 15 min. The supernatant was diluted with H_2O (0.1% trifluoroacetic acid; TFA) at a final concentration of 0.1 mg/mL analyzed by RP-HPLC. The amount of intact peptide was estimated by integrating the area under the corresponding elution peak monitored at 215 nm.

Animal Studies.—Wild-type C57BL/6J mice were purchased from the Experimental Animal Center of Chongqing Medical University (Chongqing, China). All mice were fed with standard laboratory chow, allowed free access to water, and caged at 22–24 °C with 12 h light–dark cycles. All the experiments were performed under the approved guidelines of the institutional Animal Care and Use Committee of Chongqing Medical University and the National Institute of Health guidelines on the care and use of animals were followed.

In Vivo Pharmacokinetics Studies.—Twelve 8-week-old female and male mice weighing 20–30 g were prepared and divided into three groups (4 males and 4 females in each group). PK profiles of glucagon, α /sulfonyl- γ -AApeptide hybrid analogues **15** and **19** were investigated after a single dose of 5 mg/kg (i.v). For each group, blood samples were obtained at 15 min, 30 min, 1 h, 2 h, 4 h, 8 h, and 24 h after injection by submandibular vein plexus puncture (half mice for the first 3 time points and another half for the last 4 time points to avoid ischemic shock). Blood was collected using 1.5 mL centrifuge tubes containing an anticoagulant (ethylenediaminetetraacetic acid; $\text{EDTA}\cdot 2\text{K}\cdot 2\text{H}_2\text{O}$). Plasma was separated by centrifugation at 4 °C for 10 min at 3000 g and frozen at -80 °C. Fifty microliters of standard curve samples, blank, and study plasma samples were added to 100 μL of ice-cold protein crash solvent consisting of a mixture of 9:1 vol/vol acetonitrile/glacial acetic acid. The samples were allowed to rest on ice for 15 min and centrifuged at 10,000 rpm and 4 °C for 15 min. The clarified supernatants were analyzed by LC/MS/MS.

In Vivo Pharmacodynamics Studies.—Thirty-five 8-week-old female mice with body weight in the range 20–30 g were prepared and equally divided into 7 groups. All mice were fasted for 3 h and received a single dose of insulin (0.75 IU/kg), and the blood glucose level was detected with a blood glucose monitor (OneTouch Ultra Easy, Johnson & Johnson, America). Then, mice in each group were administered with saline and 50 and 500 $\mu\text{g/kg}$ of drugs (glucagon, α /sulfonyl- γ -AApeptide hybrid analogues **15** and **19**) by intravenous

injection. The blood glucose level was detected at 15, 30, and 60 min after injection. At the end of the experiment, mice were replenished with food and water.

Supplementary Material

Refer to Web version on PubMed Central for supplementary material.

ACKNOWLEDGMENTS

The work was supported by NIH RO1AI152416 (J.C.) and NIH RO1 AG056569 (J.C.).

ABBREVIATIONS

γ-AApeptides	γ -substituted- <i>N</i> -acylated- <i>N</i> -aminoethyl peptides
GLP-1	glucagon-like peptide 1
GCGR	glucagon receptor
PEG	polyethylene glycol
DPP-4	dipeptidyl peptidase-4
cAMP	cyclic adenosine monophosphate
HTRF	homogeneous time-resolved fluorescence
CHO	Chinese hamster ovary
HEK	human embryonic kidney
MBHA	4-methylbenzhydramine
cDNA	complementary deoxyribonucleic acid
EDTA	ethylenediaminetetraacetic acid
HATU	1-[bis(dimethylamino)methylene]-1 <i>H</i> -1,2,3-triazolo[4,5- <i>b</i>]pyridinium 3-oxid hexafluorophosphate
HOBt	1-hydroxybenzotriazole
DIC	<i>N,N'</i> -diisopropylcarbodiimide
DMF	dimethylformamide
DCM	dichloromethane
EC₅₀	half-maximal effective concentration

REFERENCES

- (1). Muttenthaler M; King GF; Adams DJ; Alewood PF Trends in Peptide Drug Discovery. Nat. Rev. Drug Discov 2021, 20, 309–325. [PubMed: 33536635]

- (2). Xu D; Wu Y; Cheng Z; Yang J; Ding Y ACHP: A Web Server for Predicting Anti-Cancer Peptide and Anti-Hypertensive Peptide. *Int. J. Pept. Res. Ther* 2021, 27, 1933–1944.
- (3). Liu S; Jean-Alphonse FG; White AD; Wootten D; Sexton PM; Gardella TJ; Vilardaga J-P; Gellman SH Use of Backbone Modification to Enlarge the Spatiotemporal Diversity of Parathyroid Hormone Receptor-1 Signaling via Biased Agonism. *J. Am. Chem. Soc.* 2019, 141, 14486–14490. [PubMed: 31496241]
- (4). Liu S; Cheloha RW; Watanabe T; Gardella TJ; Gellman SH Receptor Selectivity from Minimal Backbone Modification of a Polypeptide Agonist. *Proc. Natl. Acad. Sci.* 2018, 115, 12383–12388. [PubMed: 30442659]
- (5). Cheloha RW; Maeda A; Dean T; Gardella TJ; Gellman SH Backbone Modification of a Polypeptide Drug Alters Duration of Action in Vivo. *Nat. Biotechnol.* 2014, 32, 653–655. [PubMed: 24929976]
- (6). Horne WS; Johnson LM; Ketas TJ; Klasse PJ; Lu M; Moore JP; Gellman SH Structural and Biological Mimicry of Protein Surface Recognition by α/β -Peptide Foldamers. *Proc. Natl. Acad. Sci.* 2009, 106, 14751–14756. [PubMed: 19706443]
- (7). Mbianda J; Bakail M; André C; Moal G; Perrin ME; Pinna G; Guerois R; Becher F; Legrand P; Traoré S; Douat C; Guichard G; Ochsenbein F Optimal Anchoring of a Foldamer Inhibitor of ASF1 Histone Chaperone through Backbone Plasticity. *Sci. Adv* 2021, 7, No. eabd9153.
- (8). Cussol L; Mauran-Ambrosino L; Buratto J; Belorusova AY; Neuville M; Osz J; Fribourg S; Fremaux J; Dolain C; Goudreau SR; Rochel N; Guichard G Structural Basis for α -Helix Mimicry and Inhibition of Protein-Protein Interactions with Oligoureia Foldamers. *Angew. Chem., Int. Ed.* 2021, 60, 2296–2303.
- (9). Shi Y; Sang P; Lu J; Higbee P; Chen L; Yang L; Odom T; Daughdrill G; Chen J; Cai J Rational Design of Right-Handed Heterogeneous Peptidomimetics as Inhibitors of Protein-Protein Interactions. *J. Med. Chem.* 2020, 63, 13187–13196. [PubMed: 33140956]
- (10). Sang P; Shi Y; Huang B; Xue S; Odom T; Cai J Sulfono- γ -AApeptides as Helical Mimetics: Crystal Structures and Applications. *Acc. Chem. Res.* 2020, 53, 2425–2442. [PubMed: 32940995]
- (11). Sang P; Shi Y; Higbee P; Wang M; Abdulkadir S; Lu J; Daughdrill G; Chen J; Cai J Rational Design and Synthesis of Right-Handed D-Sulfono- γ -AApeptide Helical Foldamers as Potent Inhibitors of Protein-Protein Interactions. *J. Org. Chem.* 2020, 85, 10552–10560. [PubMed: 32700908]
- (12). Sang P; Zhou Z; Shi Y; Lee C; Amso Z; Huang D; Odom T; Nguyen-Tran VTB; Shen W; Cai J The Activity of Sulfono- γ -AApeptide Helical Foldamers that Mimic GLP-1. *Sci. Adv* 2020, 6, No. eaaz4988.
- (13). Sang P; Shi Y; Lu J; Chen L; Yang L; Borchers W; Abdulkadir S; Li Q; Daughdrill G; Chen J; Cai J α -Helix-Mimicking Sulfono- γ -AApeptide Inhibitors for p53-MDM2/MDMX Protein-Protein Interactions. *J. Med. Chem.* 2020, 63, 975–986. [PubMed: 31971801]
- (14). Sang P; Zhang M; Shi Y; Li C; Abdulkadir S; Li Q; Ji H; Cai J Inhibition of β -catenin/B Cell Lymphoma 9 Protein-Protein Interaction using α -Helix-Mimicking Sulfono- γ -AApeptide Inhibitors. *Proc. Natl. Acad. Sci.* 2019, 116, 10757–10762. [PubMed: 31088961]
- (15). Teng P; Zheng M; Cerrato DC; Shi Y; Zhou M; Xue S; Jiang W; Wojtas L; Ming L-J; Hu Y; Cai J The Folding Propensity of α /Sulfono- γ -AA Peptidic Foldamers with both Left- and Right-Handedness. *Commun. Chem* 2021, 4, 58.
- (16). Shi Y; Yin G; Yan Z; Sang P; Wang M; Brzozowski R; Eswara P; Wojtas L; Zheng Y; Li X; Cai J Helical Sulfono- γ -AApeptides with Aggregation-Induced Emission and Circularly Polarized Luminescence. *J. Am. Chem. Soc.* 2019, 141, 12697–12706. [PubMed: 31335135]
- (17). Teng P; Gray GM; Zheng M; Singh S; Li X; Wojtas L; van der Vaart A; Cai J Orthogonal Halogen-Bonding-Driven 3D Supramolecular Assembly of Right-Handed Synthetic Helical Peptides. *Angew. Chem., Int. Ed.* 2019, 58, 7778–7782.
- (18). Bolarinwa O; Zhang M; Mulry E; Lu M; Cai J Sulfono- γ -AA Modified Peptides that Inhibit HIV-1 Fusion. *Org. Biomol. Chem.* 2018, 16, 7878–7882. [PubMed: 30306175]

- (19). She F; Teng P; Peguero-Tejada A; Wang M; Ma N; Odom T; Zhou M; Gjonaj E; Wojtas L; van der Vaart A; Cai J De Novo Left-Handed Synthetic Peptidomimetic Foldamers. *Angew. Chem., Int. Ed.* 2018, 57, 9916–9920.
- (20). Pereira MJ; Thombare K; Sarsenbayeva A; Kamble PG; Almby K; Lundqvist M; Eriksson JW Direct Effects of Glucagon on Glucose Uptake and Lipolysis in Human Adipocytes. *Mol. Cell. Endocrinol.* 2020, 503, No. 110696.
- (21). Åm MK; Dirnena-Fusini I; Fougner AL; Carlsen SM; Christiansen SC Intraperitoneal and Subcutaneous Glucagon Delivery in Anaesthetized Pigs: Effects on Circulating Glucagon and Glucose Levels. *Sci. Rep* 2020, 10, 13735. [PubMed: 32792580]
- (22). Thieu VT; Mitchell BD; Varnado OJ; Frier BM Treatment and Prevention of Severe Hypoglycaemia in People with Diabetes: Current and New Formulations of Glucagon. *Diabetes, Obes. Metab* 2020, 22, 469–479. [PubMed: 31820562]
- (23). Worth C; Yau D; Salomon Estebanez M; O'Shea E; Cosgrove K; Dunne M; Banerjee I Complexities in the Medical Management of Hypoglycaemia due to Congenital Hyperinsulinism. *Clin. Endocrinol.* 2020, 92, 387–395.
- (24). Banerjee I; Salomon-Estebanez M; Shah P; Nicholson J; Cosgrove KE; Dunne MJ Therapies and Outcomes of Congenital Hyperinsulinism-Induced Hypoglycaemia. *Diabet. Med.* 2019, 36, 9–21. [PubMed: 30246418]
- (25). Fremaux J; Venin C; Mauran L; Zimmer RH; Guichard G; Goudreau SR Peptide-Oligourea Hybrids Analogue of GLP-1 with Improved Action in Vivo. *Nat. Commun* 2019, 10, 924. [PubMed: 30804332]
- (26). Hager MV; Johnson LM; Wootten D; Sexton PM; Gellman SH β -Arrestin-Biased Agonists of the GLP-1 Receptor from β -Amino Acid Residue Incorporation into GLP-1 Analogues. *J. Am. Chem. Soc.* 2016, 138, 14970–14979. [PubMed: 27813409]
- (27). Johnson LM; Barrick S; Hager MV; McFedries A; Homan EA; Rabaglia ME; Keller MP; Attie AD; Saghatelian A; Bisello A; Gellman SH A Potent α/β -Peptide Analogue of GLP-1 with Prolonged Action in Vivo. *J. Am. Chem. Soc.* 2014, 136, 12848–12851. [PubMed: 25191938]
- (28). Chabenne JR; Mroz PA; Mayer JP; DiMarchi RD Structural Refinement of Glucagon for Therapeutic Use. *J. Med. Chem.* 2020, 63, 3447–3460. [PubMed: 31774682]
- (29). Yang P-Y; Zou H; Lee C; Muppidi A; Chao E; Fu Q; Luo X; Wang D; Schultz PG; Shen W Stapled, Long-Acting Glucagon-like Peptide 2 Analog with Efficacy in Dextran Sodium Sulfate Induced Mouse Colitis Models. *J. Med. Chem.* 2018, 61, 3218–3223. [PubMed: 29528634]
- (30). Lau J; Bloch P; Schäffer L; Pettersson I; Spetzler J; Kofoed J; Madsen K; Knudsen LB; McGuire J; Steensgaard DB; Strauss HM; Gram DX; Knudsen SM; Nielsen FS; Thygesen P; Reedtz-Runge S; Kruse T Discovery of the Once-Weekly Glucagon-Like Peptide-1 (GLP-1) Analogue Semaglutide. *J. Med. Chem.* 2015, 58, 7370–7380. [PubMed: 26308095]
- (31). Yang P-Y; Zou H; Chao E; Sherwood L; Nunez V; Keeney M; Ghartey-Tagoe E; Ding Z; Quirino H; Luo X; Welzel G; Chen G; Singh P; Woods AK; Schultz PG; Shen W Engineering a Long-Acting, Potent GLP-1 Analog for Microstructure-Based Transdermal Delivery. *Proc. Natl. Acad. Sci.* 2016, 113, 4140–4145. [PubMed: 27035989]
- (32). Hilger D; Kumar KK; Hu H; Pedersen MF; O'Brien ES; Giehm L; Jennings C; Eskici G; Inoue A; Lerch M; Mathiesen JM; Skiniotis G; Kobilka BK Structural Insights into Differences in G Protein Activation by Family A and family B GPCRs. *Science* 2020, 369, No. eaba3373.
- (33). Yang P-Y; Zou H; Amso Z; Lee C; Huang D; Woods AK; Nguyen-Tran VTB; Schultz PG; Shen W New Generation Oxyntomodulin Peptides with Improved Pharmacokinetic Profiles Exhibit Weight Reducing and Anti-Steatotic Properties in Mice. *Bioconjugate Chem.* 2020, 31, 1167–1176.
- (34). Lear S; Amso Z; Shen W, Chapter Eight - Engineering PEG-Fatty Acid Stapled, Long-Acting Peptide Agonists for G Protein-Coupled Receptors In *Methods in Enzymology*, Shukla AK, Ed. Academic Press: 2019; 622, 183–200. [PubMed: 31155052]
- (35). Lear S; Pflimlin E; Zhou Z; Huang D; Weng S; Nguyen-Tran V; Joseph SB; Roller S; Peterson S; Li J; Tremblay M; Schultz PG; Shen W Engineering of a Potent, Long-Acting NPY2R Agonist for Combination with a GLP-1R Agonist as a Multi-Hormonal Treatment for Obesity. *J. Med. Chem.* 2020, 63, 9660–9671. [PubMed: 32844654]

- (36). Dirnena-Fusini I; Åm MK; Fougner AL; Carlsen SM; Christiansen SC Intraperitoneal, Subcutaneous and Intravenous Glucagon Delivery and Subsequent Glucose Response in Rats: a Randomized Controlled Crossover Trial. *BMJ Open Diab. Res. Care* 2018, 6, No. e000560.
- (37). Basile A; Del Gatto A; Diana D; Di Stasi R; Falco A; Festa M; Rosati A; Barbieri A; Franco R; Arra C; Pedone C; Fattorusso R; Turco MC; D'Andrea LD Characterization of a Designed Vascular Endothelial Growth Factor Receptor Antagonist Helical Peptide with Antiangiogenic Activity in Vivo. *J. Med. Chem.* 2011, 54, 1391–1400. [PubMed: 21280635]

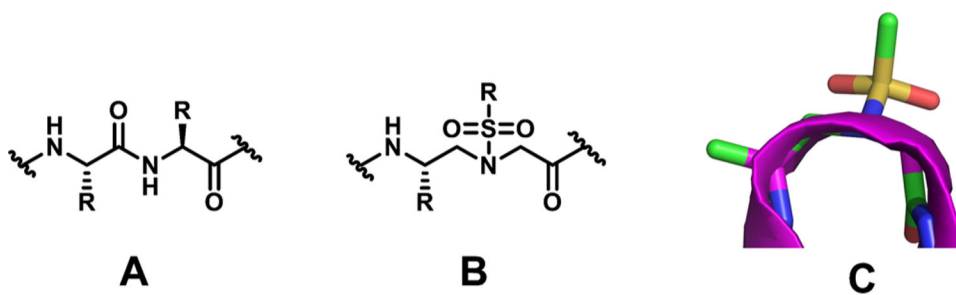


Figure 1.
(A, B) Chemical structures of α -peptide (A) and L-sulfonyl- γ -AApeptide (B); (C) Spatial structure of a sulfonyl- γ -AApeptide residue.¹⁹

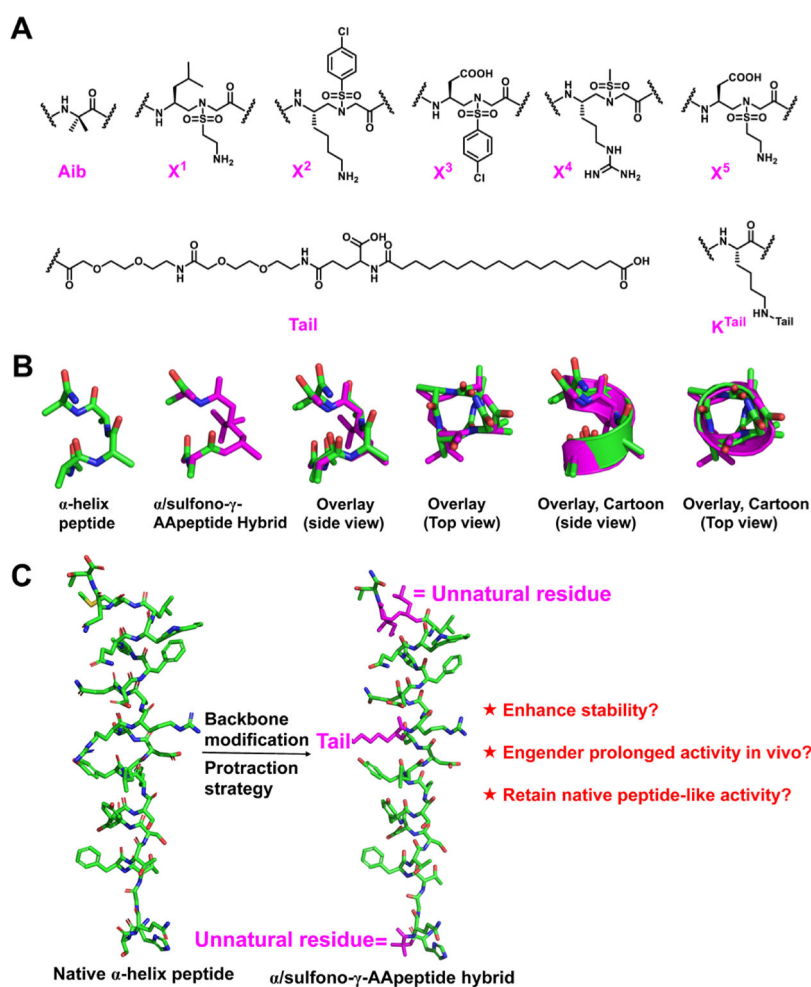


Figure 2. Structural analysis. (A) Residues employed in this study. (B) Comparison of α -helical and sulfono- γ -AApeptide backbones. (C) Design of α /sulfono- γ -AApeptide hybrid analogues of native α -helix peptides.

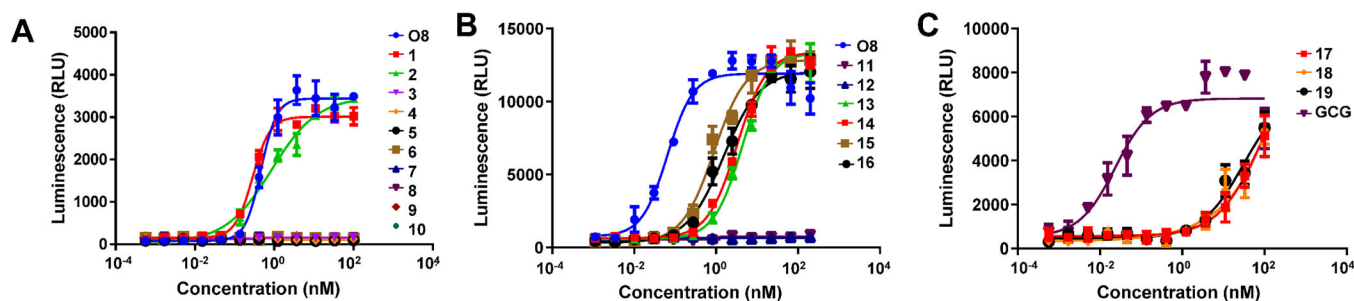


Figure 3.

(A-C) Concentration–response curves for **O8**, glucagon, and α /sulfonyl- γ -AApeptide hybrid analogues. Concentration-response curves for **O8** and α /sulfonyl- γ -AApeptide hybrid analogues to monitor the activation of GCGR; stable HEK293 cell lines with GCGR overexpression were introduced together with CRE-responsive firefly luciferase reporter (Luc) using lentivirus and selected with puromycin ($1 \mu\text{g/mL}$).

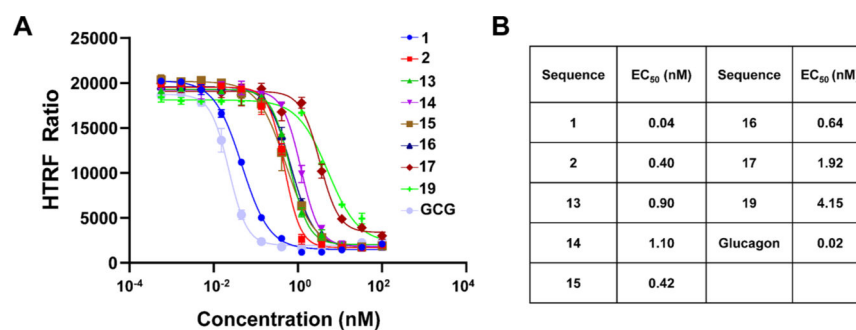


Figure 4.

(A) Concentration–response curves for glucagon and cognate α /sulfonyl- γ -AApeptide hybrid analogues. Concentration–response curves for glucagon and cognate α /sulfonyl- γ -AApeptide hybrid analogues to monitor the direct activity of cAMP activity; stable CHO-K1 cell lines with hGCGR overexpression were used. (B) Bioactivity of glucagon and lead α /sulfonyl- γ -AApeptide hybrid analogues in the cAMP assay.

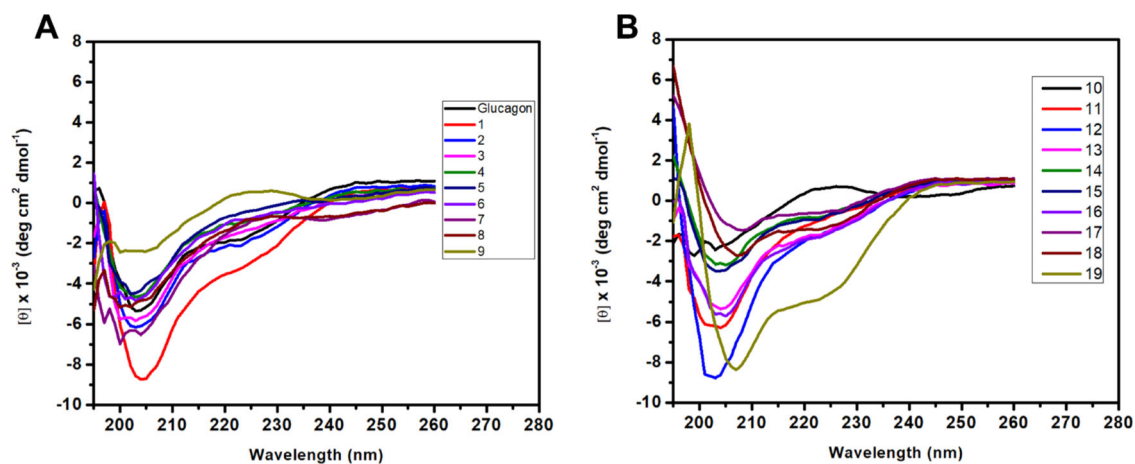


Figure 5.

(A, B) CD spectra of the regular glucagon peptide and α /sulfonyl- γ -AApeptide hybrid analogues of glucagon **1** to **19** (100 μ M) measured in phosphate-buffered saline buffer.

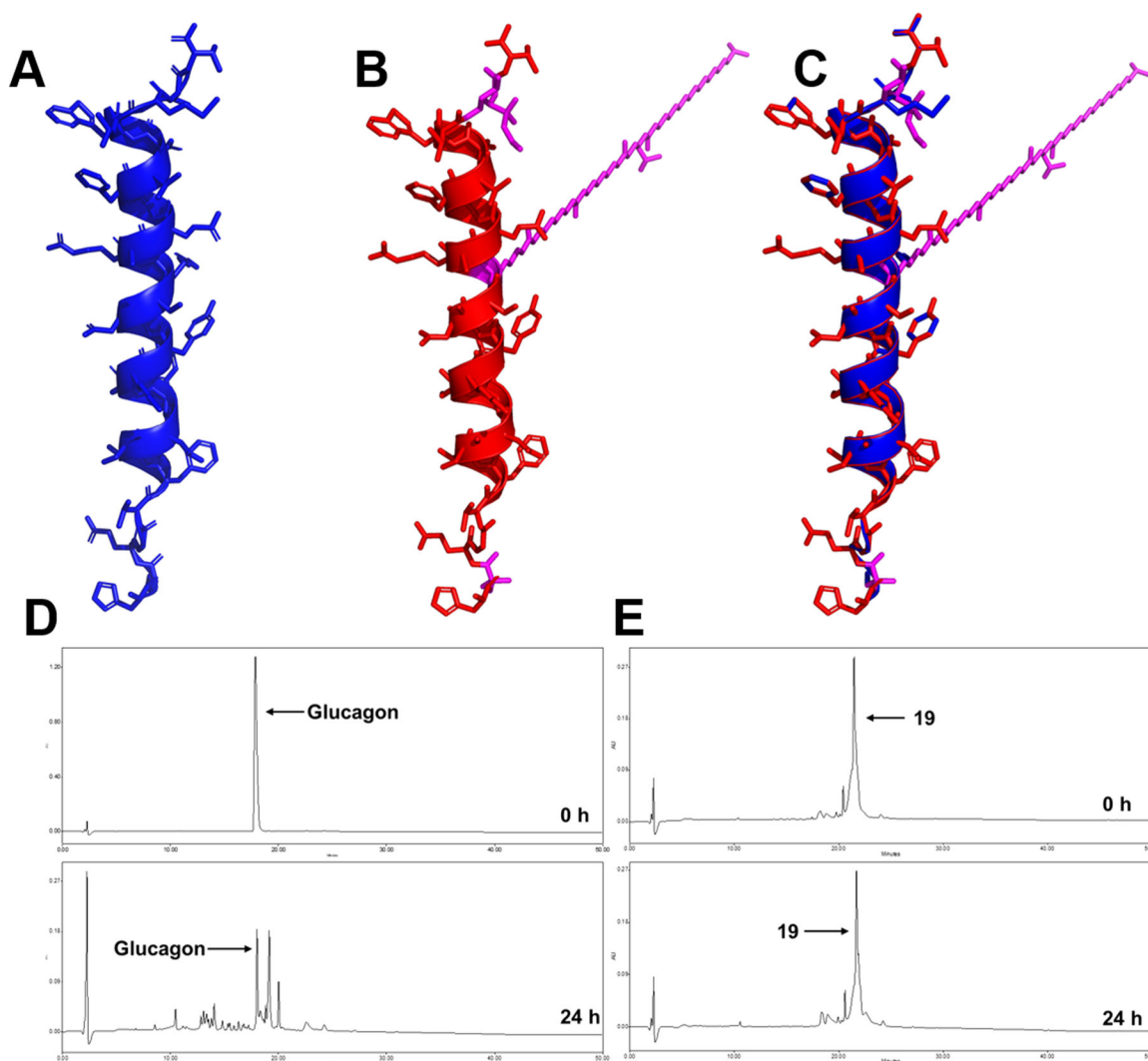


Figure 6.
(A-C) Crystal structure of glucagon (A), modeling of lead α /sulfono- γ -AApeptide hybrid **19** (B), and superimposition of glucagon with lead α /sulfono- γ -AApeptide hybrid **19** (C). (D, E) Serum stability of glucagon (D) and lead peptide **19** (E) was determined in 25% serum (v/v) at 37 °C for 24 h.

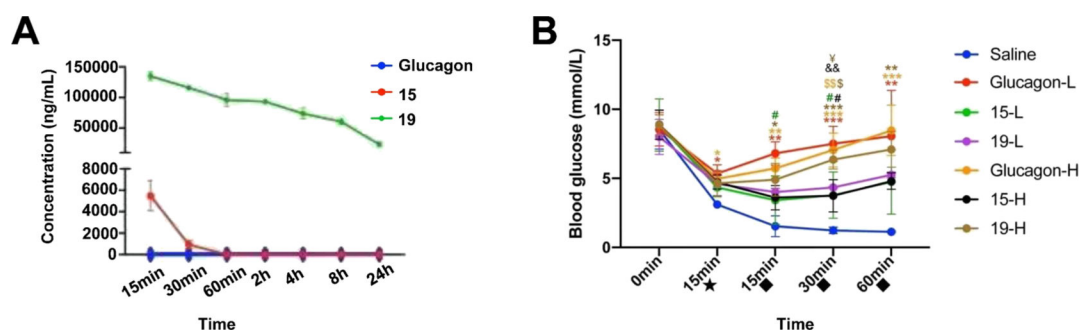
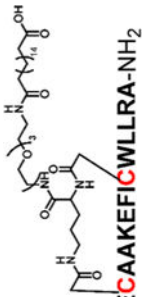


Figure 7.

(A) PK of glucagon and α /sulfono- γ -AApeptide hybrid analogues **15** and **19** (5 mg/kg, i.v) in mice over 24 h. (B) Pharmacodynamics evaluation of glucagon, **15** and **19**. Mice treated with glucagon and α /sulfono- γ -AApeptide hybrid analogues **15** and **19** (low dose 50 μ g/kg and high dose 500 μ g/kg). Data are mean \pm SD, statistical evaluation was performed using one-way ANOVA, followed by a Bonferroni test when appropriate, $n = 5$. *L* stands for low concentration; *H* stands for high concentration; ★ stands for the time after insulin injection; ◆ stands for the time after peptide injection; * $P < 0.05$, ** $P < 0.01$, *** $P < 0.001$ vs Saline; # $P < 0.05$ vs Glucagon-L; \$ $P < 0.05$, \$\$ $P < 0.01$ vs **15-L**; && $P < 0.01$ vs Glucagon-H; ¥ P vs **15-H**. The colors of *, \$, &, and ¥ correspond to each group.

Bioactivity of α /Sulfono- γ -AApeptide Hybrid Analogues in Cre Luc Production Functional Assay

Table 1.

	Sequence	EC ₅₀ (nM)	Sequence	EC ₅₀ (nM)
O8		0.46	9 H-HSQGTFTSDYSKYLX ⁵ R ⁶ X ⁷ Q ⁸ VX ³ L ⁴ X ¹ T-NH ₂	>1000
			10 Ac-HSQGTFTSDYSKYLX ⁵ R ⁶ X ⁷ Q ⁸ VX ³ L ⁴ X ¹ T-NH ₂	>1000
Glucagon	H-HSQGTFTSDYSKYLDSRRRAQDFVQWLMNT-OH	0.03	11 H-HSQGTFTSDYSKYLDSRX ⁴ QDFVQWLX ¹ T-NH ₂	>1000
1	H-HSQGTFTSDYSKYLDSRRRAQDFVQWLX ¹ T-NH ₂	0.28	12 Ac-HSQGTFTSDYSKYLDSRX ⁴ QDFVQWLX ¹ T-NH ₂	>1000
2	Ac-HSQGTFTSDYSKYLDSRRRAQDFVQWLX ¹ T-NH ₂	0.86	13 H-HGQGTFTSDYSKYLDSRRRAQDFVQWLX ¹ T-NH ₂	4.38
3	H-HSQGTFTSDYSKYLDSRRRAQDFVX ³ L ⁴ X ¹ T-NH ₂	>1000	14 Ac-HGQGTFTSDYSKYLDSRRRAQDFVQWLX ¹ T-NH ₂	3.26
4	Ac-HSQGTFTSDYSKYLDSRRRAQDFVX ³ L ⁴ X ¹ T-NH ₂	>1000	15 H-HAibQGTTFTSDYSKYLDSRRRAQDFVQWLX ¹ T-NH ₂	0.86
5	H-HSQGTFTSDYSKYLDSRRRAQX ³ VX ³ L ⁴ X ¹ T-NH ₂	>1000	16 Ac-HAibQGTTFTSDYSKYLDSRRRAQDFVQWLX ¹ T-NH ₂	1.52
6	Ac-HSQGTFTSDYSKYLDSRRRAQX ³ VX ³ L ⁴ X ¹ T-NH ₂	>1000	17 H-HAibQGTTFTSDYSKYLDSRRRAK ^{Tail} DFVQWLX ¹ T-NH ₂	77.78
7	H-HSQGTFTSDYSKYLDSRX ⁴ QX ³ VX ³ L ⁴ X ¹ T-NH ₂	>1000	18 H-HAibQGTTFTSDYSKYLDSRRRAQDFVK ^{Tail} WLX ¹ T-NH ₂	—
8	Ac-HSQGTFTSDYSKYLDSRX ⁴ QX ³ VX ³ L ⁴ X ¹ T-NH ₂	>1000	19 H-HAibQGTTFTSDYSKYLDSK ^{Tail} RAQDFVQWLX ¹ T-NH ₂	12.63